Photo-responsive disassembly of supramolecular polymer bottlebrushes in water

Luke Harvey, Jean-Michel Guigner, Laurent Bouteiller, Erwan Nicol, Olivier Colombani

ARTICLE

Photo-responsive disassembly of supramolecular polymer bottlebrushes in water

Received 00th January 20xx,
Accepted 00th January 20xx

DOI: 10.1039/x0xx00000x

Luke Harvey,[a] Jean-Michel Guigner, [b] Laurent Bouteiller[c], Erwan Nicol*[a] and Olivier Colombani*[a]

We report the 5-steps synthesis and self-assembly of an azobenzene-bisurea sticker flanked by two alkyl spacers and poly(ethylene oxide) arms. In the *trans*-azobenzene configuration, long nano-cylinders can be obtained by first molecularly dissolving the polymer in DMSO, followed by the slow addition of water. Addition of water triggers 1D self-assembly through a combination of strong, cooperative H-bonding between urea motifs and hydrophobic effect. UV-light irradiation triggers photo-isomerization of the azobenzene units to their non-planar *cis* configuration, rapidly and irreversibly disrupting the photo-responsive assemblies.

Introduction

Polymer bottlebrushes[1–5] consist of a long linear polymer backbone so densely grafted with polymer side-chains, typically on every monomer unit, that it becomes rigid and extended, affording a cylindrical (1D) morphology. The anisotropic shape and high persistence length of polymer bottle-brushes coupled with the possibility to tune their functionality and solubility by playing with the chemical structure of the side-chains makes these polymers relevant for applications in anti-fouling, nanolithography, templates for the design of inorganic nanocylinders, design of supersoft thermoplastic elastomers or medicine (drug delivery, sensing, signaling, detection). Nature also uses polymer bottlebrushes for joints lubrication, cell protection and lung clearance.[1,3,5]

Initially, polymer bottlebrushes have been prepared by covalent strategies (grafting through, grafting from or grafting to).[1,3,5] More recently, supramolecular polymer bottlebrushes[2] (SPB) have been obtained where the backbone is built by strong and directional non covalent interactions such as π-stacking or hydrogen bonding. This strategy grants more versatility to control the length, diameter and chemical functionality of the bottlebrushes compared to covalent approaches. SPB with lengths up to several hundreds of nanometers have been obtained. Additionally, the use of non-covalent interactions opens the door to the design of stimuli-responsive SPBs. Imparting stimuli-responsiveness to SPBs is of growing interest, as it broadens their applicative potential in stimuli-triggered drug delivery[6], responsive gels or emulsion stabilization[7] for example. There are however up to now very few examples of SPBs which can be disrupted in response to stimuli such as light[6], pH[8], oxidation[9–11] or host-guest interactions[12]. Moreover, most rely on the nature of the polymer arms for responsiveness, limiting versatility and applicative potential. For instance, Perrier et al. prepared light responsive SPBs where the 1D self-assembly is granted by strong cooperative hydrogen bonding in water between cyclic oligopeptides,[13] whereas the responsiveness results from the use of poly(2-nitrobenzyl methacrylate) arms. The latter become irreversibly transformed into poly(methacrylic acid) when exposed to UV irradiation, thereby triggering irreversible disassembly through electrostatic repulsion between the polymer arms.[6] This strategy clearly depends on the chemical structure of the polymer arms and does not allow modifying the chemical structure and functionality of the SPB while maintaining their responsive character.

A more versatile and attractive strategy would be to rely on the hydrogen bonding self-assembling part to impart responsiveness independently of the polymer arms. To the best of our knowledge, only five examples achieving this have been described in the literature (three examples responsive to oxidation[9–11], one to pH[14], and one based on host-guest chemistry[12]). No SPBs where the self-assembling core is light-responsive have been reported to the best of our knowledge. A few examples involving the assembly of non-polymeric small molecules in solution into 1D supramolecular structures have been described.[15–17] For instance, Feringa et. al. reported the 1D self-assembly of a stiff-stilbene functionalized with a bis-urea

[a] Institut des Molécules et Matériaux du Mans (IMMM), UMR 6283 CNRS, Le Mans Université, 72085 Le Mans, Cedex 9, France
[b] Sorbonne Université, CNRS, Institut de Minéralogie, de Physique des Matériaux et de Cosmochimie, 4 Place Jussieu, F-75005 Paris, France
[c] Sorbonne Université, CNRS, Institut Parisien de Chimie Moléculaire, Equipe Chimie des Polymères, 4 Place Jussieu, F-75005 Paris, France

Corresponding authors: erwan.nicol@univ-lemans.fr; Olivier.colombani@univ-lemans.fr

Electronic Supplementary Information (ESI) available: [details of any supplementary information available should be included here]. See DOI: 10.1039/x0xx00000x

and oligo-PEO arms in water, which proceeded through kinetic control, driven by H-bonding, π-stacking and hydrophobic effect. Assembly was so strong that photo-isomerization of assemblies of the *trans* isomer was not possible at r.t.[17] Another study reported a benzene-tricarboxamide (BTA) functionalized with azobenzene moieties, responsible for the light sensitivity and, octa-(ethylene glycol) units responsible for water solubility has been shown to undergo reversible fiber assembly/disassembly upon light irradiation.[18] However, BTAs have been reported to be unsuitable for 1D self-assembly with long polymer arms on their own,[2] requiring additional H-bonding units to drive self-assembly.[19] Indeed, 1D-supramolecular self-assembly of polymers in solution into SPBs requires very strong non covalent interactions to overcome the high entropic penalty caused by the stretching of the polymer side-chains within the SPBs,[20] a penalty that BTA are not able to overcome unless they are functionalized with short peptides; which has not been attempted in the context of light-responsive SPBs.

In the present work, we present the synthesis, characterization and supramolecular self-assembly of a poly-(ethylene oxide)-based polymer containing an azobenzene central core and urea moieties promoting the establishment of intermolecular hydrogen bonding driving the formation of SPB in aqueous solution. The effect of light (triggering the conformational switch of the azobenzene groups) on the assemblies was investigated by light scattering and cryo-electron microscopy.

Experimental section

Materials

4,4'-dihydroxyazobenzene (TCI, 98%), bromopropylamine hydrobromide (Br-C_3-NH_2.HBr, TCI, 98%), benzyl chloroformate (Acros Organics, 97%), hexamethylene diisocyanate (HMDI, Aldrich, synthesis grade), HBr in acetic acid (TCI, 30 wt.%, 5.1 mol/L), DMF (Fischer, >99%, reagent grade), dichloromethane (DCM, Carlo Erba), cyclohexane (Aldrich, >99,5%), dioxane (Honeywell, >99.5%), aqueous NaOH and HCl solutions (Aldrich), and NaOH pellets (Aldrich, 98%) were purchased and used as received. $MgSO_4$ (Fluka) and powder molecular sieves (Aldrich, 4Å) were dehydrated by heating in an oven overnight at 300°C. K_2CO_3 (Aldrich) was dried under vacuum at 40°C overnight. Deionized water was obtained using a MilliQ IQ 7000 system. Monomethoxy-hydroxy-poly-(ethylene oxide) (PEO-OH) (M_n=2000 g/mol, Đ = 1.05) was purchased from Sigma-Aldrich, and dried by azeotropic distillation using toluene. For that, a 20% wt./vol.% solution of PEO-OH in toluene was prepared, refluxed under argon for 1 hour, and toluene was then distilled off. The polymer was finally dried overnight in a vacuum oven at 50°C and stored under argon. Analytical thin-layer chromatography (TLC) was carried out using aluminium plates coated with Merck Silica gel 60 F254 (Aldrich) and observation was done under a UV lamp (254 nm). Column gel chromatography was carried out using silica gel 60 from Aldrich (SiO_2, pore size 60 Å, 40-63 µm).

Characterizations

Nuclear magnetic resonance (NMR). ^{1}H NMR spectra were recorded on either a Bruker DPX-200 or Bruker AC-400 spectrometer, using deuterated chloroform ($CDCl_3$) or dimethyl sulfoxide (DMSO-d_6) as solvents. Chemical shifts (δ) are expressed in parts per million (ppm) relative to the reference (tetramethylsilane (TMS), δ = 0 ppm). Multiplicities are reported as follows: singlet (s), doublet (d), triplet (t), quadruplet (q), quintet (qt), sextet (sext), multiplet (m), and broad signal (br s).

Size exclusion chromatography. SEC measurements in DMF were conducted on an apparatus composed of a Waters 1515 Isocratic HPLC Pump, a Waters 2707 plus Autosampler, 1 PL gel 5µm guard column and 2 PL gel 5 µm mixed-d columns (the 3 columns are stored in an oven at 60 °C), a Waters 2998 Photodiode Array Detector, a minidawn TREOS Wyatt MALS detector, a Waters 2414 Differential Refractometer (at 40 °C), using DMF with LiBr 1 g/L as eluent. The flow rate was 1 mL/min. The conventional calibration was achieved with PMMA standards polymers with apex molecular weight M_p from 904 g/mol to 304000 g/mol. Samples were prepared by dissolving the polymer in an eluent/toluene mixture (1000/1 v/v) and then filtered with 0.22 µm PTFE filters.

Light irradiations

LED irradiations were carried out using a Thor Labs DC2200 High-Power LED Driver, with Thor Labs M365LP1 and Thor Labs M450LP1 LEDs, operating at 365 nm and 450 nm, respectively. The LEDs were linked to the driver using a waveguide. Irradiation of solutions was carried out with the waveguide placed 4.5 cm above the solution. The LED irradiance at this distance was measured using a Thor Labs PM160T optical power meter, and the irradiances were measured as follows: 215 $mW.cm^{-2}$ for the 365 nm LED and 515 $mW.cm^{-2}$ for the 450 nm LED.

Cryogenic transmission electron microscopy

For cryo-TEM images, a 5 µL drop of the initial sample solution was deposited on "quantifoil"® (Quantifoil Micro Tools GmbH, Germany) carbon membrane grids. The excess of liquid on the grid was absorbed with a filter paper and the grid was quench-frozen quickly in liquid ethane to form a thin vitreous ice film using a homemade mechanical cryo-plunger. Once placed in a Gatan 626 cryo-holder cooled with liquid nitrogen, the samples were transferred in the microscope and observed at low temperature (-180 °C). Cryo-TEM images were recorded on ultrascan 1000, 2k x 2k pixels CCD camera (Gatan, USA), using a LaB_6 JEOL JEM2100 (JEOL, Japan) cryo-microscope operating at 200kV with a JEOL low dose system (Minimum Dose System, MDS, JEOL, Japan) to protect the thin ice film from any irradiation before imaging and reduce the irradiation during the image capture.

UV-Vis absorption spectroscopy

UV-Vis spectra were measured on a Jasco V760 spectrometer using glass cuvettes with an optical pathway of 1 mm at room temperature.

Light scattering

Measurements were done with a standard ALV-CGS3 system equipped with an ALV-5003 multi tau correlator system (ALV GmbH, Germany) with a vertically polarized helium-neon laser with wavelength λ = 633 nm as light source. The measurements were done at 20 °C over a large range of scattering wave vectors q varying from ca. 2.8 × 10^{-4} Å^{-1} to 2.6 × 10^{-3} Å^{-1}. $q = \frac{4\pi n}{\lambda}\sin(\frac{\theta}{2})$, with θ the angle of observation, n the refractive index of the solvent and λ = 633 nm the wavelength of the laser. The apparent hydrodynamic radius was determined by dynamic light scattering and the apparent radius of gyration and molecular weight were determined by static light scattering. It is worthy to note that samples did not absorb at 633 nm, making these solutions appropriate for LS measurements in these conditions. The dn/dc of PEO in water (0.13 mL/g) was used for Azo-(U-PEO)$_2$ in aqueous media (i.e. water/DMSO 99/ v/v).

Treatment of light scattering data.

Static light scattering (SLS). The normalized excess scattered light R, in cm^{-1}, scattered by the polymer was determined according to **Equation E1**.

$$R = \frac{R_{solution}(\theta) - R_{solvant}(\theta)}{R_{toluene}(\theta)} \times \left(\frac{n_{solvant}}{n_{toluene}}\right)^2 \times R_{toluene} \quad \textbf{E1}$$

With $R_{solution}$, $R_{solvent}$ and $R_{toluene}$ the average intensities scattered, respectively, by the solution, the solvent, and the reference (toluene) at angle θ; $n_{solvent}$ = 1.33 for water, $n_{toluene}$ = 1.496 correspond to the respective refractive indexes of water and of toluene; and $R_{toluene}$ = 1.35 × 10^{-5} cm^{-1} the Rayleigh ratio of toluene for a wavelength λ = 633 nm. For water/DMSO (99/1 v/v) solutions, $n_{solvent}$ was taken equal to n_{water}.

The normalized excess scattered light R obtained from SLS experiments depends on the polymer concentration C (in g.cm^{-3}), on a contrast factor K, on the apparent weight average molecular weight of the scatterers extrapolated to q → 0, and on a form factor P(q), which depends on the size and shape of the scatterers. The apparent molecular weight M_{app} can be approximated to the true M_w of the scatterers since interactions between scatterers may be neglected in such diluted solutions.

$$R = K \times C \times M_{app} \times P(q) \quad \textbf{E2}$$

$$K = \frac{4\pi^2 n_{solvant}{}^2}{\lambda^4 N_a} \times \left(\frac{\partial n}{\partial c}\right)^2 \quad \textbf{E3}$$

N_a is Avogadro's number and $\left(\frac{\partial n}{\partial c}\right)$ is the refractive index increment of the polymer in the chosen solvent.

Determination of the number of molecules in the cross-section. In the q-region where R/KC varies proportionally to q^{-1}, the molecular weight per unit length M_L can be determined according to equation **E4**.

$$M_L = \frac{q \times R}{\pi \times KC} \quad \textbf{E4}$$

C corresponds to the polymer concentration (g.cm^{-3}), R is the excess scattered light, K is the contrast as defined previously, and M_L is the molecular weight per unit length.

Considering that the average distance between two urea units has been reported to be 0.46 nm,[20] the number of molecules in the cross-section can be calculated according to equation **E5**.

$$\text{Number of molecules in the cross} - \text{section} = \frac{M_L \times 0.46}{M_{uni}} \quad \textbf{E5}$$

With M_{uni} the weight average molecular weight of the unimers. M_{uni} was calculated by multiplying the M_n of the unimers determined by ^{1}H NMR with their dispersity measured by SEC. $DP_{n,NMR}$ = 370/4 ≈ 92 (a total of 370 protons in the polymer chains, and 4 protons per repeat unit); $M_{n,NMR}$ = 92 x 44 + 664 ≈ 4700 g/mol (44 g/mol per repeat unit and the central core has a M = 664 g/mol), and finally M_{uni} = 4700 x 1.05 ≈ 4900 g/mol).

Dynamic light scattering (DLS). The normalized electric field autocorrelation functions ($g1(t)$) obtained by DLS measurements were analyzed in terms of a relaxation time (τ) distribution:

$$g_1(t) = \int A(\tau) e^{\left(\frac{-t}{\tau}\right)} d\tau \quad \textbf{E6}$$

The apparent diffusion coefficient D was calculated from the average relaxation rate of this relaxation mode as D = < τ^{-1} > / q^2. The apparent hydrodynamic radius R_{app} is related to D through the Stokes-Einstein equation:

$$R_{app} = \frac{k_b T}{6\pi\eta D} \quad \textbf{E7}$$

With k_b Boltzmann's constant, T the absolute temperature and η the viscosity of the solvent. When the particles are small compared to q^{-1} and the solutions are sufficiently diluted so that interactions can be neglected (i.e. at 0.9 or 1 g/L), R_{app} is equal to the z-average hydrodynamic radius, R_h.

Synthesis

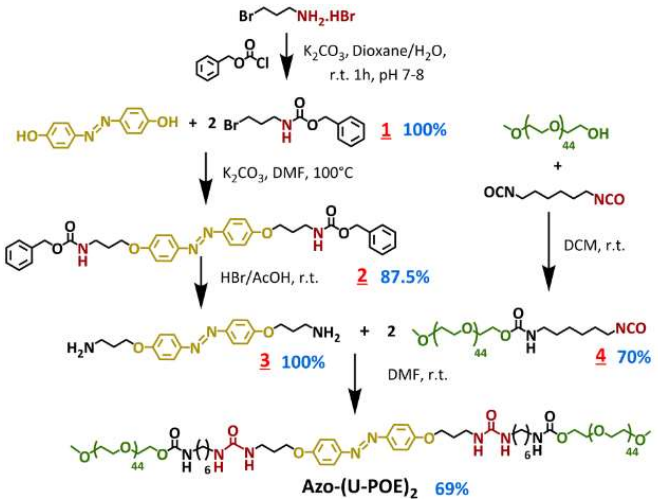

Scheme 1: **Synthetic scheme of Azo-(U-PEO)$_2$. The percentages in blue correspond to the yields of the corresponding steps.**

Synthetic protocols of azobenzenes (**1**), (**2**) and (**3**) were adapted from the literature[21] (see SI for details).

Synthesis of PEO-C_6-NCO (4)

The reaction was conducted at room temperature. In a 100 mL round bottom flask, 20 mL of anhydrous DCM was stirred under argon atmosphere with a spatula tip of activated molecular sieves (4 Å) in powder form for 30 min. Then, hexamethylene diisocyanate (HMDI, 5 eq., 1.26 g) was added to it and the solution was stirred for 30 more min. In parallel, in another (50 mL) round bottom flask, 3.00 g of dry monomethoxy-hydroxy-PEO (1.50 mmol) was solubilized in 30 mL anhydrous DCM under argon atmosphere, a spatula tip of activated molecular sieve (4 Å) in powder form was added and the solution was stirred for 30 min. The PEO-OH solution was then decanted to get rid of the molecular sieve, transferred to a 60 mL syringe, and injected into the HMDI solution over the course of 4 hours, using a syringe pump. The mixture was then left to react overnight.

The next day, the reaction mixture was concentrated without exposure to air by bubbling argon until approximately 15 mL of solution was remaining. The concentrated crude mixture was precipitated in 500 mL of anhydrous diethyl ether (DEE) under argon atmosphere and vigorous stirring, and the precipitate was then left to decant. As much supernatant as possible was removed with a canula. The vessel was filled back up with fresh anhydrous DEE, mixed, decanted, and the supernatant was removed. This operation was repeated three times in total to afford 3 washings. The precipitate was then dried under vacuum, and a white powder was obtained (2.15 g, 70 %).

It is worthy to note that this isocyanate polymer was found to be highly unstable and prone to hydrolysis, even if stored under argon at -18°C for a few days. For this reason, it was necessary to use it for the next step straight after purification. For the same reason, this polymer could not be analyzed directly by ^{1}H NMR. To verify the conversion and purity of **4**, 10 mg of the polymer was rapidly solubilized in DMSO-d_6 and a drop (large excess) of benzylamine was quickly added in order to quench the isocyanate functions by forming benzylurea moieties. The solution was then analyzed by ^{1}H NMR, revealing that the product had indeed formed quantitatively since urea peaks, alkyl peaks and the benzylic –CH_2– peak of the benzylurea were present and all integrated correctly with respect to the PEO methoxy chain end.

^{1}H NMR (DMSO-d_6, 400 MHz): δ (ppm) 6.24 (t, J_3 = 6.0 Hz, 1H), 5.88 (t, J_3 = 6.0 Hz, 1H), 4.19 (d, J_3 = 6.0 Hz, 2H), 4.04 (t, J_3 = 4.8 Hz, 2H), 3.52 (m, 180H = DP_n x 4H), 3.25 (s, 3H), 2.99 (m, 2H+2H), 1.36 (m, 2H+2H), 1.24 (m, 2H+2H).

Synthesis of Azo-(U-PEO)$_2$

In a 25 mL round bottom flask, 6 mL of dry DMF and a spatula point of molecular sieve (4 Å) in powder form were stirred under argon for 20 min. In parallel, 0.144 g (1 eq.) of azobenzene diamine **3** was solubilized in 3 mL of dry DMF with a spatula point of molecular sieve (4 Å) in powder form and stirred for 20 min. 2.00 g (2.1 eq) of PEO-C_6-NCO (**4**) were quickly added to the first solution under argon circulation. Once the polymer was solubilized, the azobenzene solution was added to the polymer solution via a syringe and was left to react for 5 min. The slight excess of isocyanate-terminated PEO was then quenched by adding 0.3 mL of benzylamine (large excess), and the reaction was left to proceed for 5 more min. The crude polymer was then precipitated in 300 mL of DEE/pentane 50/50 (v/v). ^{1}H NMR revealed that the product had indeed formed, and that no PEO-benzylurea was present. However, another side reaction seemed to have occurred, leading to the formation of an impurity (triangles on **Figure S8**). We hypothesize that the partial hydrolysis of isocyanate moieties happened, in turn leading to the formation of PEO-U-C_6-U-PEO (see **Figure S7** for details). The ^{1}H NMR spectrum showed that a third urea peak was present, representing approximately 10% of the impurity, and the specific proton signals of the product integrated systematically ~10 % lower than expected (**Figure S8**). In order to remove this unwanted impurity, 1.9 g of the crude polymer was solubilized in 2 mL EtOH, precipitated in 40 mL of DEE/EtOH 7/1 v/v, washed twice with this solvent mixture and then finally washed with pure DEE. After drying, 1.31 g of product was recovered (61 % yield), as confirmed by ^{1}H NMR (**Figure 1**), with all signals integrating as expected with the azobenzene and PEO methoxy chain end.

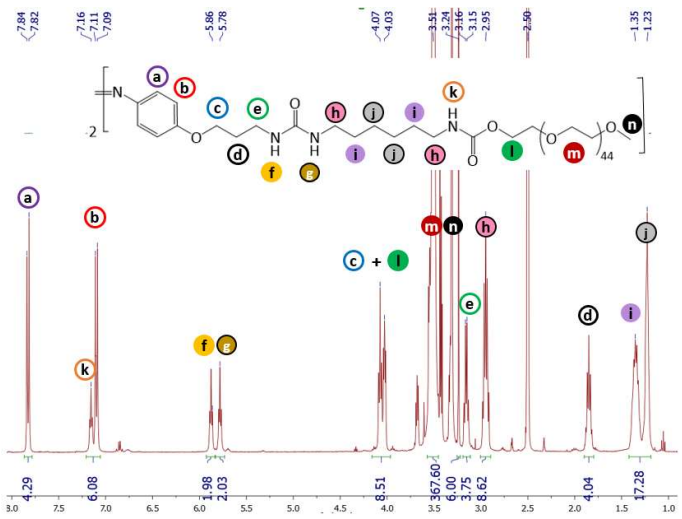

Figure 1. ^{1}H NMR (in DMSO-d_6) of the purified **Azo-(U-PEO)$_2$ (5).**

^{1}H NMR (DMSO-d_6, 400MHz): δ (ppm) 7.83 (d, **H^a**, J_3 = 9.2 Hz, 4H), 7.16 (t, **H^k**, J_3 = 5.6 Hz, 2H), 7.10 (d, **H^b**, J_3 = 9.2 Hz, 4H), 5.86 (t, **H^f**, J_3 = 6.0 Hz, 2H), 5.78 (t, **H^g**, J_3 = 6.0 Hz, 2H), 4.07 (t, **H^c**, J_3 = 6.0 Hz, 4H), 4.03 (t, **H^l**, 4H), 3.51 (s br, **H^m**, 360H = DP_n x 4H), 3.24 (s, **H^n**, 6H), 3.15 (q, **H^e**, J_3 = 6.0 Hz, 4H), 2.95 (q **H^h+H$^{h'}$**, J_3 = 6.0 Hz, 4H+4H), 1.85 (qt, **H^d**, J_3 = 6.0 Hz, 4H), 1.35 (m, **H^i+H$^{i'}$**, 4H+4H), 1.23 (m, **H^j+H$^{j'}$**, 4H+4H).

SEC measurements were carried out in DMF (and LiBr 1 g/L) with PMMA calibration. The product gave a retention time of 14.71 minutes, which corresponds to a M_n = 8300 g/mol in PMMA equivalents, which is much higher than the expected molar mass, and Đ = 1.06. Therefore, a PEO of M_n = 4000 g/mol was analyzed for comparison, and gave a similar but slightly higher retention time; which is consistent with the expected M_n

= 4700 g/mol of **Azo-(U-PEO)$_2$**. Note that there is a very slight shouldering at around 15 min retention time, which indicates that trace amounts of PEO-U-C_6-U-PEO may still be present. This is coherent with ^{1}H NMR (**Figure 1**), in which an extremely small peak at 5.70 ppm is still present, which corresponds to the PEO-U-C_6-U-PEO urea signal. The peak is however not big enough for reliable integration. It was chosen to proceed the study with this level of purity.

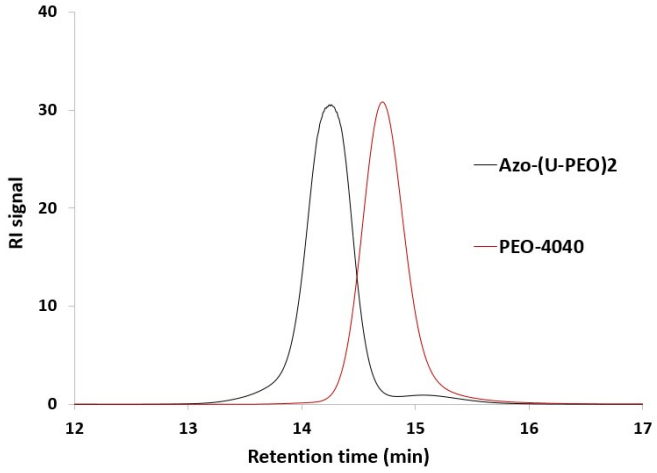

Figure 2. SEC chromatogram of the purified **Azo-(U-PEO)$_2$** and of PEO_{4k} in DMF (with LiBr 1 g/L).

Sample preparation

Direct dispersion in water. The polymer was directly dispersed at 1 g/L in ultrapure milli-Q water (which was filtered over 0.02 µm filter before use), lightly heated (approx. 40 °C) for a few minutes to accelerate dissolution, and left to stir in the dark for 1 hour. The solution was then filtered over 0.45 µm prior to LS. The loss of matter upon filtration was found to be negligible according to UV-Vis spectroscopy before and after filtration (by comparing the absorption peaks at 365 nm).

Water-DMSO route. 30 mg of polymer was solubilized in 300 µL (330 mg) of DMSO (that was filtered over 0.02 µm prior to use), heated slightly (approx. 40 °C) for a few minutes to accelerate dissolution, and left to cool to r.t. (approx. 10 min). The polymer/DMSO solution was then filtered over 0.2 µm. 200 µL of this solution were placed in a 7 mL vial, and 1.8 mL ultrapure milli-Q water (which was filtered over 0.02 µm) was added to this solution at a rate of 5 mL/h using a syringe pump, in the dark, and with a stirring of 200 rpm to reach a concentration of 9 g/L and a DMSO/water content of 10/90 v/v. 3 mL of this solution was then diluted manually by addition of water down to 0.9 g/L and a final water/DMSO ratio of 99/1 v/v. The final solution was filtered over 0.45 µm prior to light scattering measurements, and loss of matter was verified using UV-Vis (at 365 nm) and was of 8%.

Results and discussion

In order to prepare light-responsive supramolecular polymer bottlebrushes where the disruption of the self-assembled structures is controlled by the self-assembling core, we designed **Azo-(U-PEO)$_2$** (see **Scheme 1**). This approach should therefore leave the choice of polymer arms unrestrained, as long as they do not interfere with self-assembly. A bis-urea sticker,[22] which was shown to self-assemble strongly in solution, was selected as H-bond promoting unit. It was shown with small molecules that bis-ureas self-assembled several orders of magnitude more strongly than mono-ureas provided that the two urea functions were oriented in the same direction, affording a cooperative self-assembly.[22] Our strategy was therefore to separate both urea functions of **Azo-(U-PEO)$_2$** by an azobenzene moiety to impart light-responsiveness: the planar *trans* isomer should allow 1D stacking by granting cooperative self-assembly of the two urea functions, while photo-isomerization to the non-planar *cis*-azobenzene should break the cooperativity of the two urea functions and disrupt the nano-cylinders. Poly(ethylene oxide) arms (PEO, M_n=2000 g/mol per arm, Đ = 1.05) were connected on each side of the bis-urea core to impart solubility in water. These arms were linked to the core with C_6 alkyl spacers to protect the bis-ureas from H-bond competing water and reinforce the self-assembly through hydrophobic interactions.[23]

1. Synthesis of Azo-(U-PEO)$_2$

The gram-scale synthesis of **Azo-(U-PEO)$_2$** was achieved in a 5-step convergent synthesis, as described in **Scheme 1**. The critical step was the synthesis of PEO-C_6-NCO (**4**), because this required to functionalize only one function of 1,6-hexanediisocyanate by a PEO arm and to keep the remaining water-sensitive isocyanate function of (**4**) intact during purification. This was achieved by slowly adding a solution of PEO-OH to a 5-fold excess of 1,6-hexanediisocyanate in water-free conditions, followed by precipitation of the polymer in dry solvents. (**4**) was strongly moisture-sensitive and its partial hydrolysis (< 10%) occurred, requiring a selective precipitation of the final **Azo-(U-PEO)$_2$** to get rid of impurities. 1.31 g (69%) of purified **Azo-(U-PEO)$_2$** was finally obtained (see experimental section and SI for details).

2. Self-assembly of Azo-(U-PEO)$_2$ in its *trans* configuration

Next, the self-assembling properties of **Azo-(U-PEO)$_2$** were studied in aqueous medium at 1 g/L by cryoTEM and light scattering (LS). Upon direct dispersion of **Azo-(U-PEO)$_2$** in water, LS indicated a weakly aggregated system (R_h = 15 nm, N_{agg} ≈ 70, see SI, **Figure S9**), with no angular dependence, suggesting that this route does not lead to the formation of 1D assemblies. Aging the solution for 10 days did not lead to re-organization into nano-cylinders either.

A so-called "water/DMSO" route[9,24,25] was then used to favor a higher extent of aggregation: the polymer was first dissolved at high concentration in DMSO (90 g/L), a strong hydrogen bond competitor in which the polymer molecularly dissolves, followed by slow addition of water (until a final ratio of 99/1 water/DMSO (v/v) and polymer concentration of 0.9 g/L) which should trigger self-assembly.

Cryo-TEM measurements indicated that many long, polydisperse nanocylinders were present (see **Figure 3a**) confirming the targeted morphology of the self-assemblies. Additionally, some small spheres could be observed by improving the quality of the cryoTEM images (see **Figure S11** for details). Light scattering measurements confirmed the presence of nano-cylinders, since there was a q^{-1} angular dependency of the scattered intensity, characteristic of anisotropic 1D assemblies. Large dimensions (R_h = 80 nm, R_g = 140 nm) and molar mass (M_w = 4.10^6 g/mol, corresponding to an aggregation number $N_{agg} \approx 800$) confirmed the large extent of aggregation compatible with the formation of long nanocylinders (see **Figure 3c**). LS measurements were also used to determine the number of molecules self-assembled within the cross-section of the nanocylinders. For that purpose R.q/KCπ was plotted as a function of q, revealing the formation of a plateau at high q (**Figure S14**), corresponding to M_L with a value of $9.0x10^3$ $g.mol^{-1}.nm^{-1}$ (calculated using **Equation E4** as explained in the experimental section). Using **Equation E5**, the number of molecules in the cross-section was calculated to be 1.0. The data were fitted using Sasview (see **Figure 3c**, red curve), with an average length of 520 nm and a diameter of 10 nm, which is consistent with cryo-TEM ($L \approx 500$ nm). Considering the distance of a fully stretched PEO monomer unit of 0.28 nm[26] and an Azo core length around 2 nm, stacked **Azo(-U-PEO)$_2$** molecules with fully stretched PEO_{44} arms should lead to nanocylinders with a diameter of 27 nm ($d_{stretched}$ = 0.28 x 44 x 2 + 2). The smaller experimental diameter of the nanocylinders implies that the PEO_{44} arms in the self-assemblies are stretched approximately to one third of their maximum length, which seems reasonable for SPBs decorated by neutral polymer arms. As long as the azobenzene units were in their *trans* configuration, the "DMSO-route" therefore successfully led to the formation of long, thin and isolated SPBs consisting of **Azo-(U-PEO)$_2$** stacked upon each other by hydrogen bonds and protected from bundling by the polymer arms. Since direct dispersion in water hardly led to assembly, the strong influence of the preparation pathway indicates that the system is kinetically frozen (i.e. out of thermodynamic equilibrium), which was also observed with similar systems in aqueous medium.[9,24,25] Acetone and ethanol were also used as potential subsitutes for DMSO (see **Figure S16** for details) to prepare SPBs with the "DMSO-like preparation route", but did not yield nano-cylinders. This could be due to the fact that while these solvents are good H-bond competitors, they are bad solvents for the self-assembling core, whereas DMSO is a good solvent. Therefore they probably do not allow molecular solubilization of **Azo-(U-PEO)$_2$** as unimers prior to water addition; which prevents its well-organized assembly into supramoecular SPBs.

3. Light response of the self-assemblies

The light responsiveness of **Azo-(U-PEO)$_2$** was studied both by UV-Vis to determine whether the *trans* → *cis* isomerization occurred, and by cryoTEM and LS to determine the consequence it had on the self-assembled structures. Initially, the polymer contained almost 100% *trans*-azobenzene (<3% *cis*) according to ^{1}H NMR (see **Figure 1,** the aromatic peaks at 7.83 and 7.10 ppm correspond to the *trans*-azobenzene protons). Irradiation under gentle stirring of a 0.9 g/L "water/DMSO" (99/1) solution at 365 nm resulted in the progressive decrease of the absorption band at 365 nm, corresponding to the π → π* transition of *trans*-azobenzene, and a simultaneous appearance of two absorption bands at 315 nm and 450 nm corresponding respectively to the π → π* and n → π* transitions of *cis*-azobenzene (**Figure 4a**).[27] Visually, the solution turned a deeper orange, allowing for direct macroscopic observation of the isomerization. The *trans* → *cis* isomerization therefore occurs, and is rather quick, with the photo-stationary state being reached after only a few minutes and corresponding to a *trans*/*cis* molar ratio of 25/75 (according to ^{1}H NMR, see **Figure S19** for details).

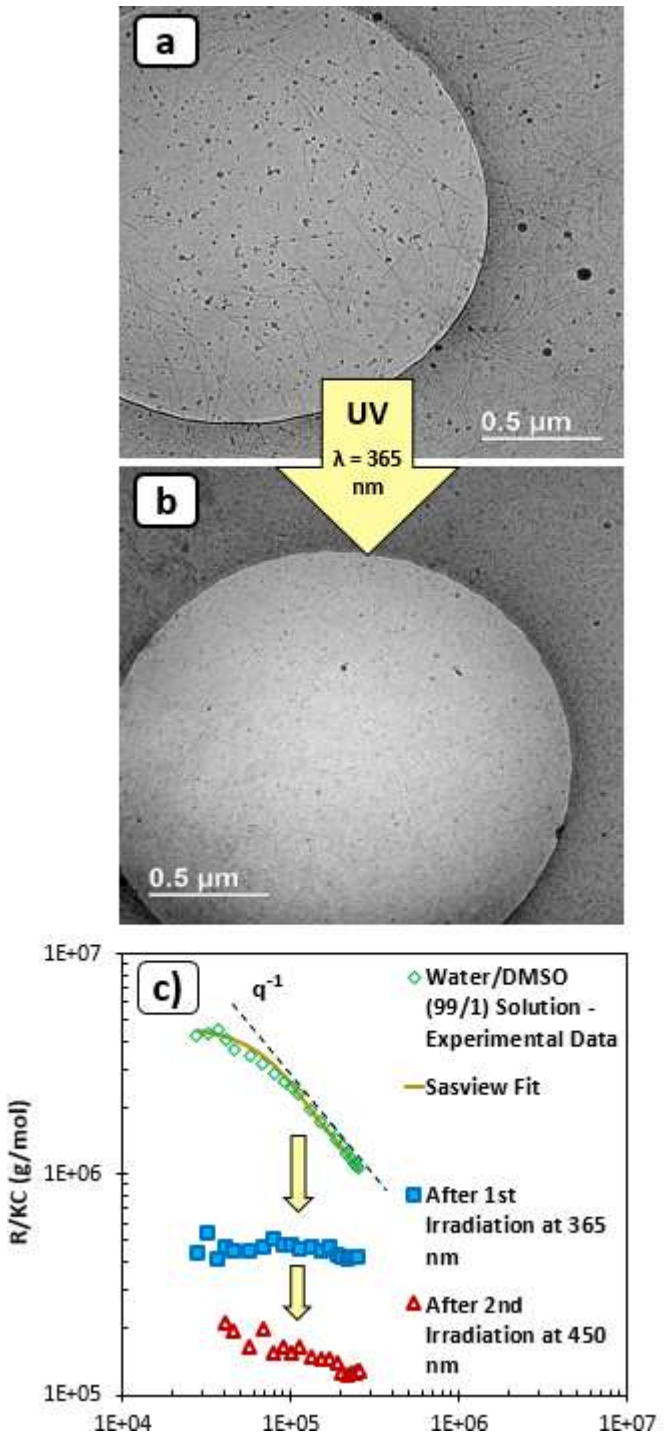

Figure 3. Cryo-TEM images using the water/DMSO route (at 0.9 g/L) **(a)** before UV irradiation - and **(b)** after UV irradiation (λ = 365 nm). The large highly contrasted black dots are ice crystals. **(c)** R/KC ratio as a function of q measured by SLS prior to irradiation (green diamonds, the data were fitted using Sasview, with L = 520 nm, r = 5 nm, —), after UV irradiation at λ = 365 nm (blue squares), and after a second irradiation at λ = 450 nm (red triangles). The black dotted line is a q^{-1} visual aid.

Subjecting the latter solution to irradiation at 450 nm allowed reappearance of the *trans* absorption band and disappearance of the *cis* ones. The new stationary state was reached within a minute (see **Figure 4b**) and corresponded to a *trans*/*cis* ratio of 75/25 by mol (according to ^{1}H NMR, see **Figure S19**). 100% of *trans* isomer could not be achieved by irradiation at 450 nm; which was attributed to the fact that both *cis* → *trans* and *trans* → *cis* isomerization are triggered at this wavelength, the quantum yield for the latter transition being much lower, but not negligible.[18] It was verified that 365 nm/450 nm irradiation cycles led to identical ratios of isomers, indicating no degradation occurs (see **Figure 4c**). Moreover, heating a *cis*-rich solution at 80°C for 30 minutes led again to an amount of *trans*-isomer close to 100% through thermal relaxation (see **Figure S18** for details). Thermal relaxation also occurred at r.t., but it was rather slow ($\tau_{1/2} \approx 22$ hours) (see **Figure S17** for details).

To conclude, *trans* → *cis* and *cis* → *trans* photo-induced isomerization occurred very rapidly and reversibly in aqueous medium even though the polymer was involved in 1D supramolecular structures. It was additionally verified that photo-isomerization occurs on a similar timescale in aqueous medium after direct dispersion in water (photo-stationary states being reached within a matter of minutes), where **Azo-(U-PEO)$_2$** weakly assembles and forms spherical particles (see **Figure S10** for details). This implies that the *trans* → *cis* photo-isomerization is not strongly hindered by the self-assembly of **Azo-(U-PEO)$_2$** into 1D structures. This result is quite relevant as it has been reported that self-assembly into fibers may prevent photo-isomerization in some cases,[17,28] although this is not systematic.

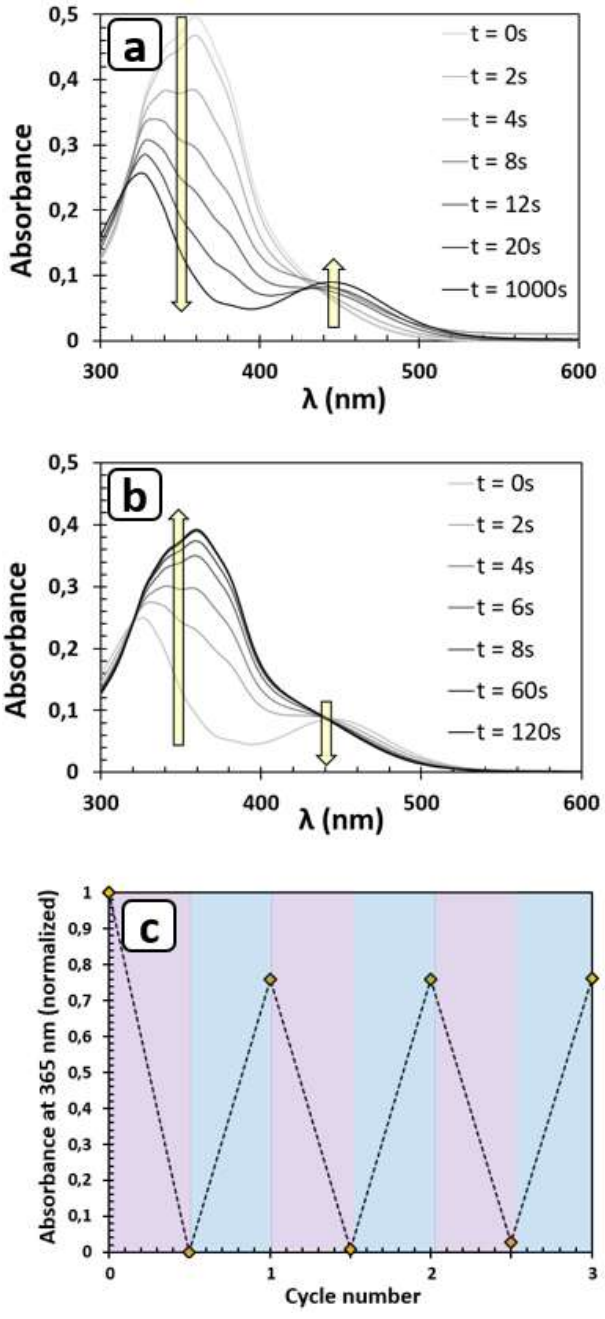

Figure 4. (a) *Trans* →*Cis* photo-isomerization (365 nm) of Azo-(U-PEO)$_2$,**(b)** *Cis* → *Trans* photo-isomerization (450 nm) of Azo-(U-PEO)$_2$ and **(c)** Photo-isomerization cycles of Azo-(U-PEO)$_2$, (at 0.9 g/L following the "water/DMSO" route)

To probe the effect of photo-isomerization on the assemblies, a solution prepared by the "water/DMSO" route was irradiated at 365 nm and analyzed by cryo-TEM and LS (see **Figure 3b** and **3c**) revealing disruption of the nanocylinders: $N_{agg} \approx 90$, $R_h = 40$ nm, no more angular dependency of the scattered intensity. The still large N_{agg} and R_h however suggest that the cylinders are not fully disrupted into unimers but into small objects, which may be spheres and/or small bits of the initial nanocylinders (see **Figures 3b and S12** which indeed reveals the presence of small spherical particles as well as a few very short 1D structures).

Further irradiating at 450 nm triggered isomerization back to *trans*-azobenzene as mentioned above, but was not accompanied by the re-assembly of nano-cylinders (see **Figure 3c**). Actually, irradiating at 450 nm even led to a decrease in assembly ($N_{agg} = 30$, $R_h = 15$ nm), and cryo-TEM revealed that only small spherical particles were present. These latter particles are similar to those obtained with **Azo-(U-PEO)$_2$** in its trans configuration by direct dispersion in water (see above). To confirm that the cis-isomer does not self-assemble into 1D structures, a "water/DMSO" solution was prepared by irradiating with UV-light (365 nm) the initial DMSO solution to form *cis*-**Azo-(U-PEO)$_2$** before adding water. LS indicated weak aggregation ($N_{agg} = 20$, $R_h \sim 15$ nm) with no q^{-1} angular dependence (see **Figure S15**), confirming that *cis*-**Azo-(U-PEO)$_2$** cannot form nanocylinders even with the "water/DMSO" route. We actually note that the self-assembled structures formed in these conditions are even less aggregated than those obtained upon irradiation at 365 nm of a solution of nanocylinders of *trans*-**Azo-(U-PEO)$_2$** ($N_{agg} \approx 90$, $R_h = 40$ nm). This suggests that *cis*-**Azo-(U-PEO)$_2$** also formed out-of-equilibrium structures with pathway-dependent characteristics.

From these results, we hypothesize that both the preparation pathway and the configuration of the azobenzene units influence the organization of the polymer as depicted on **Figure 5**.

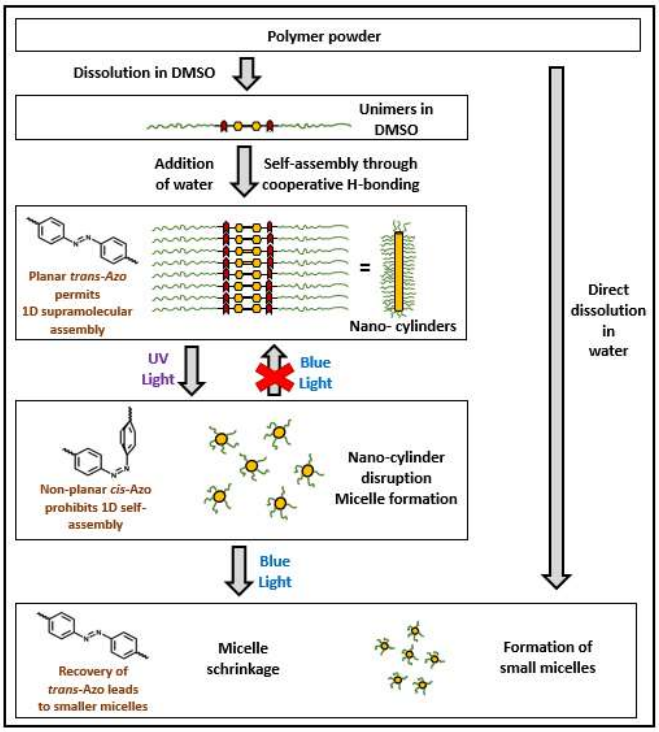

Figure 5. Schematic representation of the physico-chemical behavior of **Azo-(U-PEO)$_2$** in water following the "water/DMSO" route.

The *cis*-**Azo-(U-PEO)$_2$** apparently disfavors the formation of long nanocylinders, as expected, because it certainly suppresses the cooperative hydrogen bonding of both urea functions for geometrical reasons, thereby leading to relatively weak

hydrogen bonds. The *trans*-**Azo-(U-PEO)$_2$** may lead to the formation of long nanocylinders thanks to cooperative hydrogen bonding, but only with certain preparation conditions, namely the "DMSO-route". Indeed, the "DMSO-route" allows the initial dissolution of **Azo-(U-PEO)$_2$** as unimers, which probably helps them stack one on top of the other through directional and cooperative hydrogen bonds when water is added. In these conditions, hydrogen bonding is probably the main driving force for the formation of elongated supramolecular nanocylinders, the hydrophobic interactions only playing a protecting role over the hydrogen bonds from H-bond competing water. Now, if *trans*-**Azo-(U-PEO)$_2$** is obtained by irradiating at 450 nm a solution of small spherical micelles of *cis*-**Azo-(U-PEO)$_2$**, it starts from a supramolecular organization mainly driven by hydrophobic interactions which are not directional. Those hydrophobic interactions probably disfavor for kinetic reasons the reorganization of the *trans*-**Azo-(U-PEO)$_2$** into hydrogen bonded stacks of molecules required to reform nanocylinders. It should be noted that some examples in the literature report weakly dynamic assemblies which slowly evolve from spheres to elongated structures over time. It could therefore have been expected that the transition from *cis* back to *trans* might lead again to nanocylinders after prolonged time. However, direct dispersion of *trans*-**Azo-(U-PEO)$_2$** did not lead to nanocylinders even after ten days; suggesting a strong kinetic hurdle preventing self-assembly of *trans*-**Azo-(U-PEO)$_2$** into 1D structures unless starting with unimers as enabled by the "DMSO-route".

The *cis*-*trans* isomerization of **Azo-(U-PEO)$_2$** therefore does not allow the reformation of nanocylinders. Still, changing the configuration of the azobenzene units from *cis* to *trans* seems to slightly impact the packing parameter of the molecules, which would explain why spherical particles of *cis*-**Azo-(U-PEO)$_2$** become slightly less aggregated upon irradiation at 450 nm into *trans*-**Azo-(U-PEO)$_2$**. This argument is further supported by the fact that the micelles of *trans*-**Azo-(U-PEO)$_2$** have roughly the same characteristics as those obtained by direct dispersion in water. A similar variation of the aggregation state of micelles upon *cis*-*trans* isomerization was reported in the literature for an azobenzene-urea terminated PEO, which underwent an increase in micelle radius upon UV irradiation.[29]

Conclusions

To summarize, we report the successful synthesis of **Azo-(U-PEO)$_2$**, a polymer which combines a self-assembling bis-urea sticker with a photo-responsive azobenzene core and PEO polymer arms. This compound can self-assemble in aqueous medium into long SPBs following an appropriate strategy ("water/DMSO route"). The use of rather long PEO arms affords the formation of very thin and isolated nanocylinders (diameter ~ 10 nm) formed by mono-molecular hydrogen-bonded stacks of **Azo-(U-PEO)$_2$** in the cross-section of the nanocylinders and no significant lateral aggregation. The very high specific surface area and aspect ratio of these particles makes them potentially relevant for applications as Pickering emulsion stabilizers or to interact with biological material such as DNA or proteins.

Exposing the nanocylinders to UV irradiation at 365 nm rapidly triggers photo-isomerization to *cis*-azobenzene, which in turn provokes the disruption of the nanocylinders. This represents the first light-sensitive SPB where the light-responsiveness is intrinsic to the self-assembling core rather than to the specificity of the polymer arm. This may allow changing the functionality and chemistry of the polymer arms without losing their response to light. Further irradiating at 450 nm rapidly triggers photo-isomerization back to the *trans* isomer, but does not lead to nano-cylinder reassembly, which could be explained by the frozen character of the assemblies in water. Efforts are thus required in the future to develop reversibly-responsive SPBs.

Acknowledgments

Le Mans Université is acknowledged for funding LH's PhD work. The authors thank Sandra Kalem and Clémence Nicolas for fruitful discussions. Anthony Rousseau and Frédérick Niepceron and plateforme "Microscopy" at IMMM are thanked for their help with cryo-TEM measurements, Boris Jacquette and platerforme "Matière molle" are thanked for SEC measurements, and Sullivan Bricaud and plateforme "RMN" are thanked for help with NMR measurements.

Conflicts of interest

There are no conflicts to declare.

Notes and references

1 R. Verduzco, X. Li, S. L. Pesek and G. E. Stein, *Chem Soc Rev*, 2015, **44**, 2405–2420.

2 F. V. Gruschwitz, T. Klein, S. Catrouillet and J. C. Brendel, *Chemical Communications*, 2020, **56**, 5079–5110.

3 S. S. Sheiko, B. S. Sumerlin and K. Matyjaszewski, *Progress in Polymer Science (Oxford)*, 2008, **33**, 759–785.

4 M. Zhang and A. H. E. Müller, *J Polym Sci A Polym Chem*, 2005, **43**, 3461–3481.

5 S. Tu, C. K. Choudhury, I. Luzinov and O. Kuksenok, *Curr Opin Solid State Mater Sci*, 2019, **23**, 50–61.

6 J. Yang, J. I. Song, Q. Song, J. Y. Rho, E. D. H. Mansfield, S. C. L. Hall, M. Sambrook, F. Huang

and S. Perrier, *Angewandte Chemie - International Edition*, 2020, **59**, 8860–8863.

7 J. Tang, P. J. Quinlan and K. C. Tam, *Soft Matter*, 2015, **11**, 3512–3529.

8 S. C. Larnaudie, J. C. Brendel, K. A. Jolliffe and S. Perrier, *ACS Macro Lett*, 2017, **6**, 1347–1351.

9 C. Nicolas, T. Ghanem, D. Canevet, M. Sallé, E. Nicol, C. Gautier, E. Levillain, F. Niepceron and O. Colombani, *Macromolecules*, 2022, **55**, 6167–6175.

10 R. Otter, C. M. Berac, S. Seiffert and P. Besenius, *Eur Polym J*, 2019, **110**, 90–96.

11 J. Baram, E. Shirman, N. Ben-Shitrit, A. Ustinov, H. Weissman, I. Pinkas, S. G. Wolf and B. Rybtchinski, *J Am Chem Soc*, 2008, **130**, 14966–14967.

12 Q. Song, J. Yang, J. Y. Rho and S. Perrier, *Chemical Communications*, 2019, **55**, 5291–5294.

13 Q. Song, Z. Cheng, M. Kariuki, S. C. L. Hall, S. K. Hill, J. Y. Rho and S. Perrier, *Chem Rev*, 2021, 121, 13936–13995.

14 R. Otter, K. Klinker, D. Spitzer, M. Schinnerer, M. Barz and P. Besenius, *Chemical Communications*, 2018, **54**, 401–404.

15 M. Gerth, J. A. Berrocal, D. Bochicchio, G. M. Pavan and I. K. Voets, *Chemistry - A European Journal*, 2021, **27**, 1829–1838.

16 S. Lee, S. Oh, J. Lee, Y. Malpani, Y. S. Jung, B. Kang, J. Y. Lee, K. Ozasa, T. Isoshima, S. Y. Lee, M. Hara, D. Hashizume and J. M. Kim, *Langmuir*, 2013, **29**, 5869–5877.

17 F. Xu, S. Crespi, L. Pfeifer, M. C. A. Stuart and B. L. Feringa, *CCS Chemistry*, 2022, **4**, 2212–2220.

18 E. Fuentes, M. Gerth, J. A. Berrocal, C. Matera, P. Gorostiza, I. K. Voets, S. Pujals and L. Albertazzi, *J Am Chem Soc*, 2020, **142**, 10069–10078.

19 T. Klein, H. F. Ulrich, F. V. Gruschwitz, M. T. Kuchenbrod, R. Takahashi, S. Fujii, S. Hoeppener, I. Nischang, K. Sakurai and J. C. Brendel, *Polym Chem*, 2020, **11**, 6763–6771.

20 S. Catrouillet, C. Fonteneau, L. Bouteiller, N. Delorme, E. Nicol, T. Nicolai, S. Pensec and O. Colombani, *Macromolecules*, 2013, **46**, 7911–7919.

21 W. Wei, T. Tomohiro, M. Kodaka and H. Okuno, 2000, 8979–8987.

22 V. Simic, L. Bouteiller and M. Jalabert, *J Am Chem Soc*, 2003, **125**, 13148–13154.

23 E. Obert, M. Bellot, L. Bouteiller, F. Andrioletti, C. Lehen-Ferrenbach and F. Boué, *J Am Chem Soc*, 2007, **129**, 15601–15605.

24 T. Choisnet, D. Canevet, M. Sallé, C. Lorthioir, L. Bouteiller, P. Woisel, F. Niepceron, E. Nicol and O. Colombani, *ACS Nano*, 2021, **15**, 2569–2577.

25 S. Han, S. Pensec, D. Yilmaz, C. Lorthioir, J. Jestin, J. M. Guigner, F. Niepceron, J. Rieger, F. Stoffelbach, E. Nicol, O. Colombani and L. Bouteiller, *Nat Commun*, 2020, **11**, 2–7.

26 C. Darko, (2018), "An Experimental Approach of Introducing Polymer Crystallization to Students using Diblock Copolymer Thin Films", The University of Manchester, V1, DOI: 10.17632/hry2mscm54..

27 M. Baroncini and G. Bergamini, *Chemical Record*, 2017, **17**, 700–712.

28 D. Inoue, M. Suzuki, H. Shirai and K. Hanabusa, *Bull Chem Soc Jpn*, 2005, **78**, 721–726.

29 S. Yadav, S. R. Deka, G. Verma, A. K. Sharma and P. Kumar, *RSC Adv*, 2016, **6**, 8103–8117.

